

Dark matter distribution in simulated Milky Way analogs

Maria C. Cavalcante-Siviero¹ & K. Menéndez-Delmestre²

¹ Brazilian Center for Research in Physics (CBPF) e-mail: mariaclara@cbpf.br

² Valongo Observatory, Federal University of Rio de Janeiro (OV/UFRJ); e-mail: kmd@astro.ufrj.br

Abstract. Each galaxy is immersed in a dark matter (DM) halo, subject to dynamic interactions and evolutionary changes across cosmic time. The density of DM in galaxies can vary according to the size of the halo in which the galaxy is located. In this work we use the Illustris TNG, a suite of state-of-the-art cosmological galaxy formation simulations, to study the distribution of DM in galaxies similar to the Milky Way (MW). We built a sample of simulated MW analogs, using the maximum rotation speed (V_{max}) and star formation rate (SFR) as selection criteria. This allows us to limit the systems to late-type galaxies, which are characterized by active star formation, and to choose DM halos with total masses similar to that of the MW. Using mass distribution maps of stars, DM and gas provided by TNG50, we built radial profiles of each of these components and explored the mass distribution within each galaxy, focusing on DM. One of our goals is to constrain the DM density in the Solar neighborhood of the MW, based on DM density measurements at the equivalent Solar distance in the galaxies of our sample. We calculate the DM density at the corresponding location in the Solar neighborhood ($1.6 \times R_{eff}$) in each MW analog and obtain a DM density of $\rho_{DM} \sim 0.01 M_{\odot} pc^{-3}$ at the equivalent Solar location. Our results are consistent with recent work on rotation curves (RC) based on atomic hydrogen (HI) observations for small (<10) samples of MW-like galaxies, as well as more traditional estimates based on measurements within our own MW. Taking advantage of the size of our sample of simulated galaxies, we have also set out to study the “galaxy-halo” connection, with a view to exploring trends between the global properties of these systems and the DM distribution.

Resumo. Cada galáxia está imersa em um halo de matéria escura (DM), sujeita a interações dinâmicas e mudanças evolutivas ao longo do tempo cósmico. A distribuição de DM nas galáxias pode variar de acordo com o tamanho do halo no qual a galáxia está localizada. Neste trabalho, usamos o Illustris TNG, um conjunto de simulações cosmológicas de formação de galáxias de última geração, para estudar a distribuição de DM em galáxias análogas à Via Láctea (VL). Criamos uma amostra de galáxias análogas simuladas, usando a velocidade máxima de rotação (V_{max}) e a taxa de formação de estrelas (SFR) como critérios de seleção. Isso nos permite limitar os sistemas a galáxias do tipo tardio, que são caracterizadas pela formação ativa de estrelas, e escolher halos de DM com massas totais semelhantes à da VL. Usando mapas de distribuição de massa estelar, DM e gás disponibilizados pelo Illustris TNG50, construímos perfis radiais de cada um desses componentes e exploramos a distribuição de massa ao longo de toda a extensão da galáxia, com foco na DM. Um dos objetivos de nosso projeto é restringir a densidade de DM na vizinhança Solar da VL, com base nas medidas de densidade de DM na distância Solar equivalente nas galáxias de nossa amostra. Calculamos a densidade de DM no local correspondente da vizinhança Solar ($1.6 \times R_{eff}$) em cada uma das galáxias análogas e obtemos uma densidade local de DM de $\rho_{DM} \sim 0.01 M_{\odot} pc^{-3}$ na posição Solar equivalente. Nossos resultados são consistentes com trabalhos recentes de curvas de rotação baseados em observações de hidrogênio atômico (HI) para amostras pequenas (<10) de galáxias análogas à VL. Aproveitando o tamanho de nossa amostra de galáxias simuladas, iniciamos também um estudo da conexão “Galáxia-Halo”, visando explorar tendências entre propriedades globais destes sistemas e a distribuição de DM.

Keywords. Dark matter – Galaxies: spiral – Galaxies: halos – Galaxies: structure

1. Introduction

The standard cosmological model, Λ CDM, predicts that dark energy and dark matter (DM) dominate the mass and energy density of the Universe (Planck Collaboration et al. 2020). Over the years, efforts have been made to estimate the DM distribution in our own galaxy, the Milky Way (MW; e.g., Iocco et al. 2011; Nesti & Salucci 2013; Posti & Helmi 2018). Although rotation curves (RC) are often used to study DM in external galaxies, calculating the DM distribution for the MW is not a simple task. Studying analog galaxies helps us with this challenge.

In recent decades, several experiments have been carried out with the aim of detecting massive DM particles through their interactions with ordinary matter or indirectly through their annihilation products Aprile et al. 2017; Aalbers et al. 2023. The leading hypothesis is that non-baryonic DM consists of neutral weakly interacting massive particles (WIMPs), which were created in the hot early Universe, decoupled from ordinary matter and have survived to this day Steigman & Turner (1985). Measuring these events would provide information on the mass and probability of interaction of DM with ordinary matter. In

order to generate predictions of the expected number of DM detection events, these DM detection experiments on Earth need to know estimates of the DM density at our Galactic address. Theoretical and empirical models are being developed to increasingly constrain this value. So far, the nature and detailed spatial distribution of DM continues to elude our understanding.

We adopted a cosmology Λ -CDM plane geometry with $H = 67.74 [km s^{-1} Mpc^{-1}]$, $\Omega_{\Lambda,0} = 0.6911$, $\Omega_{m,0} = 0.3089$, $\Omega_{b,0} = 0.0486$, $\sigma_8 = 0.8159$ and $n_s = 0.9667$ (Pillepich et al. 2019).

2. Our MW analog sample

Investigating the distribution of DM within the MW presents a unique challenge, as our position within the Galaxy makes it difficult to interpret observational data. To overcome this limitation, one effective approach is to study MW analog galaxies, as they provide an external perspective on similar dynamical and structural properties (Salucci et al. 2007). With this in mind, we choose galaxies from the IllustrisTNG-50 cosmological simu-

lations¹ (hereafter TNG50: Pillepich et al. 2019; Nelson et al. 2019), to explore the DM distribution in systems that closely resemble our own Galaxy. The simulation relies on the hydrodynamic treatment of the gas, which extends into a cubic volume of ≈ 50 Mpc lateral length.

To build a sample of simulated MW analog galaxies, we based our selection criteria on the maximum rotation speed (V_{max}) - which allows us to choose DM halos with total masses similar to that of our Galaxy; and on the star formation rate (SFR) - with the aim of limiting the systems to spiral galaxies, which are characterized by active star formation (Kennicutt et al. 1989; Leroy et al. 2013), similar to the MW. In summary, we selected our sample of MW analog galaxies at redshift $z = 0$ (TNG50 Snapshot 99), using the following criteria:

1. $1.0 M_{\odot} \text{ yr}^{-1} < SFR < 8.5 M_{\odot} \text{ yr}^{-1}$ (based on the reference value for the MW; Elia et al. 2022);
2. $200 \text{ km s}^{-1} < V_{max} < 315 \text{ km s}^{-1}$ (based on the reference value for the MW; Reid et al. 2016; Eilers et al. 2019).

Applying these criteria, our parent halo of simulated MW analog galaxies consist of 141 systems.

2.1. Selecting cosmological subhalos

According to Iocco et al. (2011), microlensing data and observations of the internal dynamics of MW-like galaxies show a DM density profile consistent with that of Navarro, Frenk & White (NFW; Navarro et al. 1996, 1997) and Einasto (1965). In this work we expect to reproduce a radial profile that resembles these models and, consequently, better fits the observational data.

We identify that certain systems in our sample present very high stellar-to-DM mass ratios (M_{\star}/M_{DM}). By applying a cutoff ($M_{\star}/M_{DM} < 0.5$), we eliminate 14 systems with little or no DM particles². This result in a final sample of 127 MW analogs. Figure 1 shows the range in stellar mass ($1 < M_{\star} [M_{\odot} 10^{10}/h] < 12$) and DM mass ($\sim 10 < M_{DM} [M_{\odot} 10^{10}/h] < 300$) present in our sample. The values for the stellar and DM mass in the MW were estimated based on recent literature (Karukes et al. 2019).

2.2. Mass distribution maps

Using 2D distribution maps of stars, gas and DM mass, we investigate the mass profiles of each component as a function of radius (Fig. 2). We seek to derive DM densities at the corresponding Solar location in these galaxies. Similar studies, based on a handful of MW analogs observed in HI (de Isídio et al. 2024) undertake this work based on the decomposition of RCs to isolate the DM component. Based on a sample of simulated MW analogs that is $20 \times$ larger we seek results that can be directly compared to observational works. For that reason, we first manipulate our TNG50 2D distribution maps of stars, DM and gas to reflect a resolution comparable to that of observational work. With this in mind, we consider the typical resolution of images at the wavebands used to trace each component. In the case of stellar maps, we reproduce the image quality acquired with IRAC data from Spitzer observations (e.g., *Spitzer Survey*

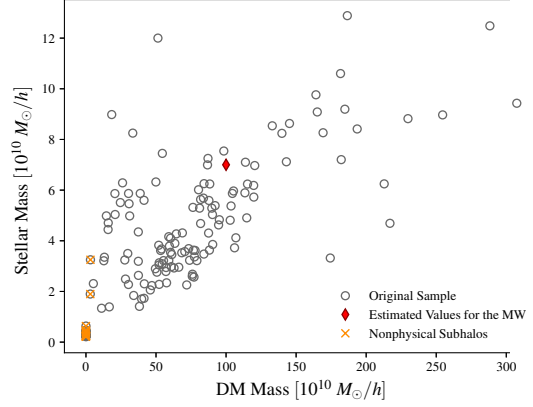


FIGURE 1. Distribution of stellar and DM masses present in our sample of 141 MW analogs, with the corresponding values for the MW (red diamond; Licquia & Newman 2015; Karukes et al. 2019). The 14 systems with no cosmological origin are shown as orange crosses (see text for details). Our final sample of 127 MW analogs is shown as black circles.

of Stellar Structures in Galaxies, S4G; Sheth et al. 2010) and use an angular resolution of $1.3''$ at a physical distance of 20 Mpc . In the case of gas and DM maps, we use an angular resolution of $10''$ (de Isídio et al. 2024) at the same distance.

3. Radial DM density profile

3.1. Solar neighborhood

One of our main goals is to provide an analogy between our sample of simulated galaxies and the MW, in order to estimate a range of values of what the DM density would typically be for MW-type galaxies in the region corresponding to the Solar neighborhood. The distance between the Sun and the center of the MW is $\sim 8 \text{ kpc}$ (Ghez et al. 2008; Reid et al. 2014), which corresponds to 1.6 times the effective radius R_{eff} ³ of the MW, where $R_{eff} = 5 \text{ kpc}$ based on the value for the MW’s disc scale-length suggested by Licquia & Newman (2015). To construct a representative density profile for the simulated galaxies, we require a standard distance proportional to each galaxy’s size. By assuming a constant mass-to-light ratio (M/L) ratio, we ensure that the sphere containing half of the luminosity also contains half of the mass. As simulations work with mass distributions rather than light, we adopt a standardized distance of $1.6 \times R_{half}^{\star}$, where R_{half}^{\star} ⁴ readily provided by TNG50 for each galaxy. This approach enables us to “translate” the position of the Sun for each of the TNG-50 MW analogs.

TNG50 resolution adopts a fixed value for the smallest unit of DM mass [$3.1^{-5} M_{\odot} 10^{10}/h$], hence, to find the total DM mass we have to multiply the size involved in the region by the DM mass value. We calculate the DM mass inside spherical shells from the center of the galaxies (the mass radial profile is exhibited in Fig. 3). To compute the volume, we assume a spherical symmetry⁵ for the shape of the DM halo and apply a thickness

¹ <https://www.tng-project.org>

² We attribute these close-to-zero DM halos as potential results of galaxy mergers from which “chunks” of stellar mass were separated from their parent halos. These TNG50 subhalos, although they comply with our main selection criteria, appear to be environments in which all the DM was removed. We refer to these systems as systems with no cosmological origin and we exclude them from our analysis.

³ R_{eff} is the effective radius, the radius enclosing half of a galaxy’s total light at a given band.

⁴ R_{half}^{\star} represents the radius enclosing half of the stellar mass.

⁵ The shape of DM halos is generally predicted to be non-spherical, as it is influenced by the non-spherical nature of the Gaussian density peaks in the primordial density field from which the halos originate

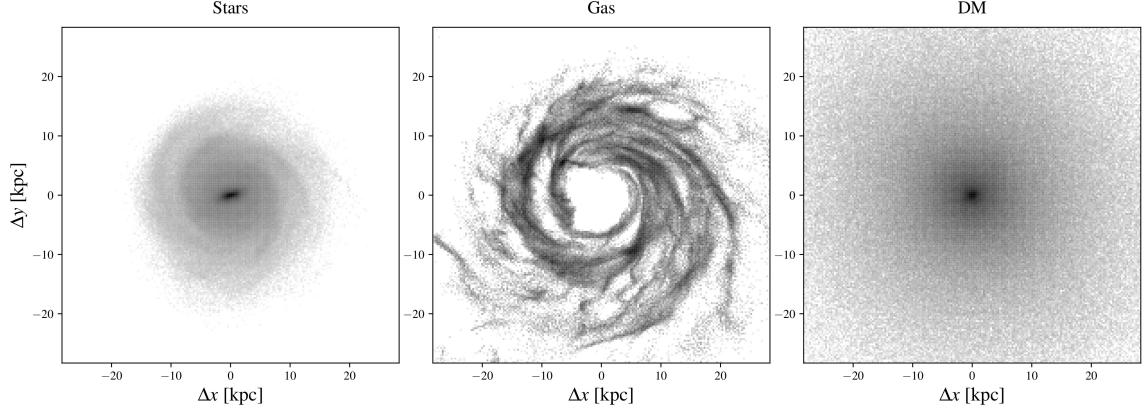


FIGURE 2. Two-dimensional maps of stellar (left), gas (middle) and DM (right) distribution for subhalo 63869.

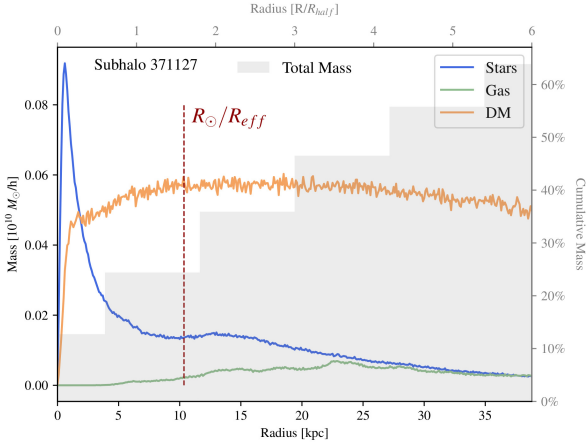


FIGURE 3. Radial mass profile for each component of the subhalo 371127: stars (blue), gas (green) and DM (orange). The equivalent position of the Sun is marked in red, at $1.6 \times R_{eff}$ (see text for details). The bar graph (light gray) shows the accumulated mass in relation to the total mass.

of 0.1 kpc to the spherical shells. This allows us to estimate the DM density specifically in the region of interest, once we have defined the Solar neighborhood in these systems. In Fig. 4, we present the DM distribution of our sample of simulated galaxies and that of 5 nearby MW analogs observed in HI analyzed in de Isídio et al. (2024).

3.2. Mock rotation curves

The standard structure used to describe spiral galaxies consists of a central bulge, a stellar disk, an extended gaseous disk and a spherical DM halo. Studying the RC of a galaxy and decomposing it into its different components is a powerful means to derive the mass distribution in a late-type galaxy. RCs enable us to constrain the size and mass of the DM halo.

The velocity dispersion observed in emission lines (e.g., H α , HI, CO) through spectroscopic measurements is typically insignificant when compared to the rotational velocity of a spiral

(Doroshkevich 1970). The presence of a baryonic disk is also believed to influence the shape of DM halos (Machado & Athanassoula 2010). Yet, a spherical symmetry is still a good approximation for calculating the enclosed mass, especially in the inner region of these systems (Hussein et al. 2025; Velmani & Paranjape 2025).

galaxy (Sofue 2016). Therefore, it is reasonable to balance gravitational and centrifugal forces¹, given the negligible contribution of the pressure term in the virial theorem:

$$\frac{m V^2}{r} = \frac{G M m}{r^2} \therefore V \propto r^{-\frac{1}{2}} \quad (1)$$

With the radial mass profiles in hand, we can easily generate mock RCs for our sample considering the contribution of the different components, as follows:

$$V_c(r) = \sqrt{V_\star(r)^2 + V_{gas}(r)^2 + V_{DM}(r)^2} \quad (2)$$

where $V_\star(r)$, $V_{gas}(r)$ and $V_{DM}(r)$ correspond, respectively, to the stellar, gas and DM contributions to the circular velocity $V_c(r)$.

The RC shape typically observed in spiral galaxies is characterized by a steep rise in velocities within the central region, followed by an approximately constant velocity beyond a certain galactocentric distance (Bosma 1981; Sofue & Rubin 2001). To model this behavior, we present in Fig. 5 a single mock RC that incorporates contributions from stars, gas, and DM. By combining these components, we derive the final circular velocity profile $V_c(r)$ for the system, which successfully reproduces the observed RC features—rapidly increasing velocities in the inner region and a flattening at larger distances.

3.3. Local dark matter density

Based on the DM density profiles of our MW analog sample (Fig. 4), we obtain a range of values for the DM density at the equivalent Solar distance ($1.6 \times R_{eff}$) with a median value of $0.01 \text{ M}_\odot \text{ pc}^{-3}$ (see Fig. 6). This is consistent with results presented by a wealth of other studies focused on measurements of the MW itself and a few select others with an observational focus on a handful of MW analogs (e.g., de Isídio et al. 2024); see Tab. 1 for a summary of these works. This consistency reinforces the validity and power of using external galaxies as analog laboratories to study the DM distribution within a galaxy like the MW.

4. Galaxy-halo connection

Halos are regions of gravitationally bound matter that have collapsed as a result of the expansion of the Universe (White & Rees 1978). These objects host internal structures called subhalos, which in turn can host galaxies when they have enough

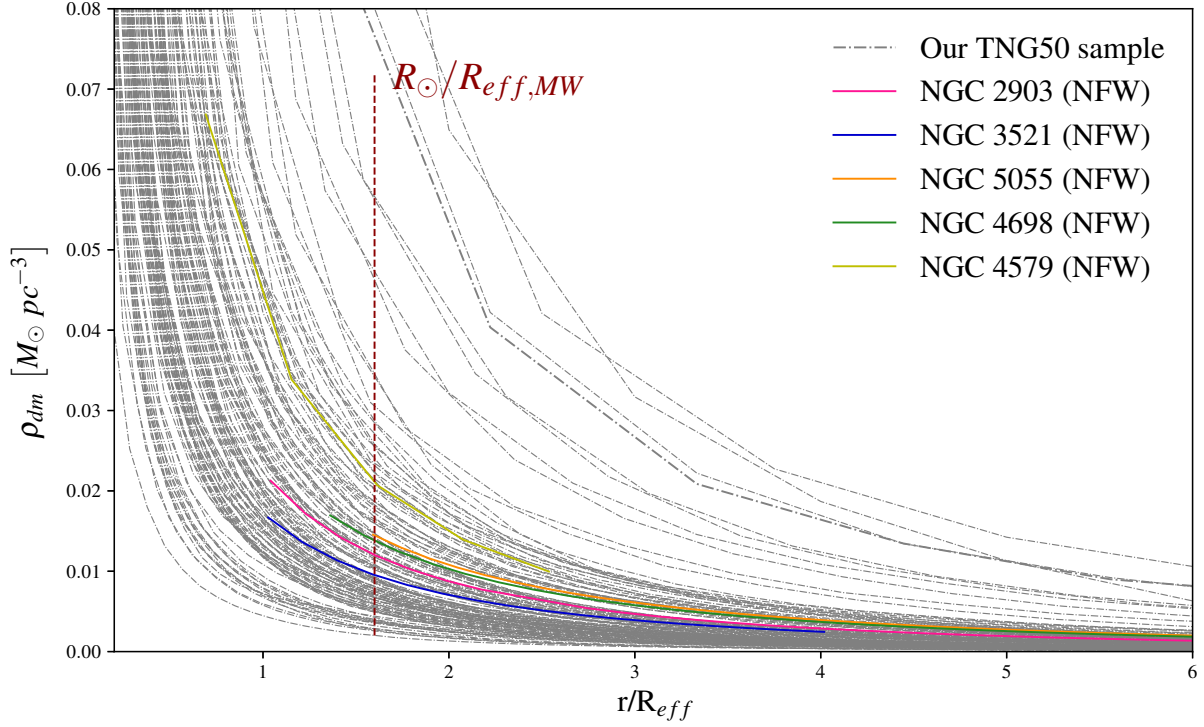


FIGURE 4. DM density profile for our sample of 127 simulated MW analog galaxies (dotted gray) and 5 nearby MW analogs observed in HI (solid colors; de Isídio et al. 2024) as a function of radius normalized by the R_{eff} .

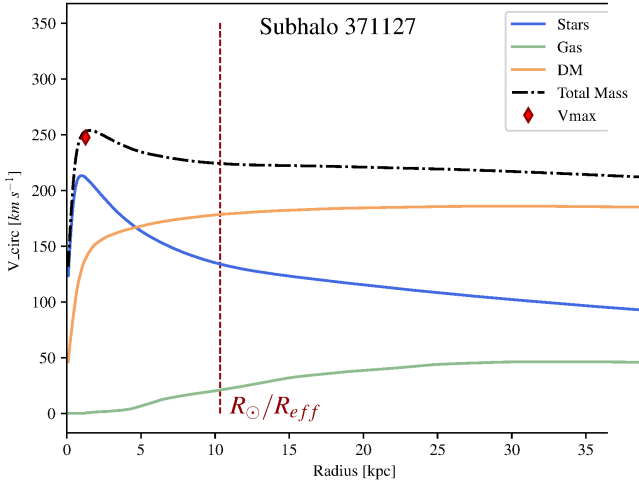


FIGURE 5. Mock RC for the subhalo 371127: $V_{\star}(r)$, $V_{gas}(r)$, $V_{DM}(r)$, $V_{c,total}(r)$, respectively, in blue, green, orange and dash-dotted black.

mass to form them (Wechsler & Tinker 2018). According to Barnes & Hernquist (1996), galaxies are self-gravitating systems of stars, gas and DM “particles”. We have seen that each galaxy is immersed in a DM halo, which undergoes various interactions and modifications over cosmic time. The connection between the galaxy and the DM halo is a key point for this analysis.

Many authors have been searching ways to associate what type of galaxy occupies what kind of halo, especially in terms of relative mass. This is usually done with numerical algorithms

TABLE 1. Local DM density estimates for different authors.

Authors	Local DM density	
	$M_{\odot} pc^{-3}$	$GeV cm^{-3}$
<i>Standard Halo Model (SHM)</i>	0.008	0.30
Salucci et al. (2010)	0.008 - 0.015	0.32 - 0.54
Weber and de Boer (2010)	0.005 - 0.01	0.20 - 0.40
Iocco et al. (2011)	0.005 - 0.015	0.20 - 0.56
Bovy and Tremaine (2012)	0.008 - 0.011	0.20 - 0.40
Nesti & Salucci (2013)	0.012 - 0.013	0.41 - 0.52
Sofue (2015)	0.008 - 0.011	0.18 - 0.42
Pato & Iocco (2015)	0.008 - 0.013	0.30 - 0.50
Eilers et al. (2019)	0.008	0.27 - 0.33
Karukes et al. (2020)	0.012 - 0.013	0.40 - 0.46
Pillepich et al. (2024)	0.005 - 0.013	0.20 - 0.50
de Isídio et al. (2024)	0.005 - 0.014	0.21 - 0.55
This Work	0.010	0.37

(e.g. Berlind & Weinberg 2002; Dolag et al. 2009). The Illustris TNG suite employs two types of halo and subhalo matching algorithms, Friends-of-Friends (FOF; Huchra & Geller 1982) and the SUBFIND group finder (Springel et al. 2001). The former relies on spatial criteria to assign galaxies to groups, while halos are identified with the latter, which recognizes self-bonded substructures in a catalog of FOF halos. In the simulation context, this means that we can access the mass information of a halo and its substructures, and directly infer a hierarchical mass relationship for any system. In Fig. 7 we show the galaxy-halo connection for our MW analog sample. We are interested in exploring how the DM distribution is associated with other global

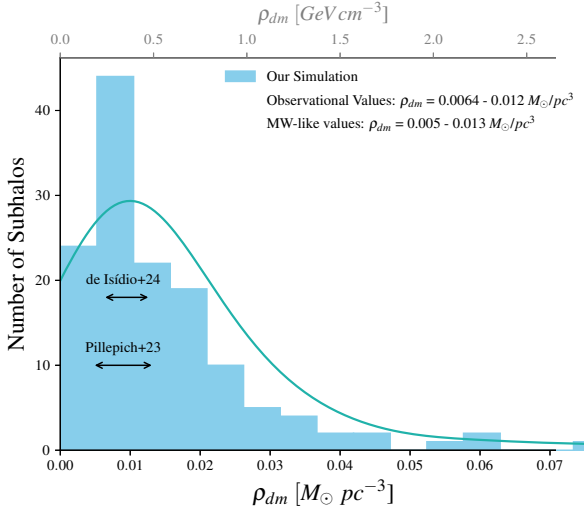


FIGURE 6. Histogram of the local density of DM. We apply a Gaussian fit to the data and obtain $\rho_{DM} = 0.01 M_{\odot} pc^{-3}$. We highlight two intervals from the literature (de Isídio et al. 2024; Pillepich et al. 2024), and note that our median agrees with both references.

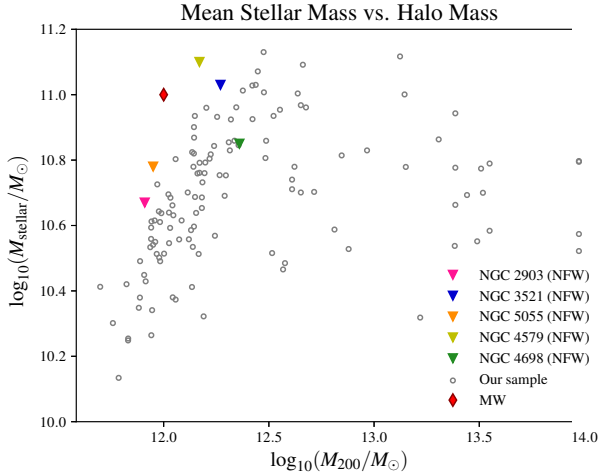


FIGURE 7. Stellar-to-halo mass relation for our sample of MW analogs (black circles) and for 5 nearby MW analogs observed in HI (solid colors; de Isídio et al. 2024).

properties of our MW analogs. We are just starting to tackle this analysis.

5. Conclusions

In this work we study the distribution of DM in MW analog galaxies using the TNG50 cosmological simulation. Our approach focuses on calculating the DM density at the radial distance equivalent to the Sun’s position in the MW, at $1.6 \times R_{half}^*$, considering the effective radius of each of these analogs. Recent studies based on significantly smaller samples (e.g., <10 ; de Isídio et al. 2024) of galaxies with high-resolution HI data ($<10''$) allow us to immediately put these results into context. The success of our results demonstrates the potential of using cosmological simulations to characterize the distribution of DM in MW analog galaxies. Our work can also benefit DM direct experiments on Earth by proving a narrow range of DM density values to estimate the MW’s local DM density.

Despite being a worthwhile selection of MW analogs within a general framework, our sample could be further improved. Our current sample was not based on morphological parameters (due to the lack of such a morphological catalog at the time); we thus cannot attest to the unequivocal disk-nature of the galaxies in our sample. This means that some of the objects may correspond to other galaxy types within Hubble’s classification (e.g., elliptical, irregular; Hubble 1926). We argue that these objects represent a small part of the original sample (roughly 10%) and their inclusion should not impact with the main results of this work.

Acknowledgements. MCCS thanks the support of the Brazilian National Research Council (CNPq), as well as the Brazilian Center for Research in Physics (CBPF). KMD thanks the support of the Serrapilheira Institute (grant Serra-1709-17357), as well as that of the Brazilian National Research Council (CNPq grant 308584/2022-8) and of the Rio de Janeiro Research Foundation (FAPERJ grant E-32/200.952/2022), Brazil.

References

- Aalbers, J., Akerib, D. S., Akerlof, C. W., et al. 2023, *PhRvL*, 131, Art.id. 041002.
- Aprile, E., Aalbers, J., Agostini, F., et al. 2017, *PhRvL*, 119, 181301.
- Barnes, J. E., Hernquist, L. 1996, *ApJ*, 471, 115.
- Berlind, A. A., Weinberg, D. H. 2002, *ApJ*, 575, 587.
- Bosma, A. 1981, *AJ*, 86, 1825-1846.
- Bovy, J., Tremaine, S. 2012, *ApJ*, 756, 89.
- de Isídio, N. G. et al. 2024, *ApJ*, 971, 69.
- Dolag, K. et al. 2009, *MNRAS*, 399, 497.
- Doroshkevich, A. G. 1970, *Astrophysics*, 6, 320.
- Einasto, J. 1965, *TrAlm*, 5, 87.
- Elia, D. et al. 2022, *ApJ*, 941, 162.
- Eilers, A.-C. et al. 2019, *ApJ*, 871, 120.
- Ghez, A. M. et al. 2008, *ApJ*, 689, 1044.
- Hubble, E. P. 1926, *ApJ*, 64, 321.
- Huchra, J. P., Geller, M. J. 1982, *ApJ*, 257, 423.
- Hussein, A., Necib, L., Kaplinghat, M., et al. 2025, *arXiv:2501.14868*.
- Iocco, F. et al. 2011, *JCAP*, 2011, 029.
- Karukes, E. V., Benito, M., Iocco, F., Trotta, R., Geringer-Sameth, A. 2019, *arXiv:1912.04296 [astro-ph.GA]*.
- Kennicutt, R. C. et al. 1989, *ApJ*, 344, 685.
- Leroy, A. K. et al. 2013, *AJ*, 146, 19.
- Licquia, T. C., Newman, J. A. 2015, *ApJ*, 806, 96.
- Machado, R. E. G., Athanassoula, E. 2010, *MNRAS*, 406, 2386.
- Marinacci, F. et al. 2018, *MNRAS*, 480, 5113.
- Navarro, J. F., Frenk, C. S., White, S. D. M. 1996, *ApJ*, 462, 563.
- Navarro, J. F. et al. 1997, *ApJ*, 490, 493.
- Nelson, D., Pillepich, A., Springel, V., et al. 2019, *MNRAS*, 490, 3234.
- Nelson, D. et al. 2018, *MNRAS*, 475, 624.
- Nesti, F., Salucci, P. 2013, *JCAP*, 2013, 016.
- Pato, M., Iocco, F. 2015, *ApJL*, 803, L3.
- Piffl, T., Binney, J. et al. 2014, *MNRAS*, 445, 3133.
- Pillepich, A. et al. 2019, *MNRAS*, 490, 3196.
- Pillepich, A. et al. 2024, *MNRAS*, 535, 1721.
- Planck Collaboration, Akrami, Y., Arroja, F., et al. 2020, *A&A*, 641, A10.
- Posti, L., Helmi, A. 2018, *arXiv:1805.01408*.
- Reid, M. J. et al. 2014, *ApJ*, 783, 130.
- Reid, M. J. et al. 2016, *ApJ*, 823, 77.
- Salucci, P., Lapi, A., Tonini, C., et al. 2007, *arXiv:astro-ph/0703115*.
- Salucci, P. et al. 2010, *A&A*, 523, A83.
- Sheth, K. et al. 2010, *PASP*, 122, 1397.
- Sofue, Y., Rubin, V. 2001, *ARA&A*, 39, 137.
- Sofue, Y. 2015, *PASJ*, 67, 75.
- Sofue, Y. 2016, *arXiv:1608.08350*.
- Springel, V. et al. 2001, *MNRAS*, 328, 726.
- Springel, V. et al. 2018, *MNRAS*, 475, 676.
- Steigman, G., Turner, M. S. 1985, *Nucl. Phys. B*, 253, 375.
- Velmani, P., Paranjape, A. 2025, *JCAP*, 02, 006.
- Weber, M., de Boer, W. 2009, *arXiv:0910.4272*.
- Wechsler, R. H., Tinker, J. L., 2018, *ARA&A*, 56, 435. doi:10.1146/annurev-astro-081817-051756
- White, S. D. M., Rees, M. J. 1978, *MNRAS*, 183, 341.